

Manuscript Number: ICARUS-13573R2

Title: A multi-scale magnetotail reconnection event at Saturn and associated flows: Cassini/UVIS observations

Article Type: Special Issue: Saturn's Auroral Campaign

Keywords: Saturn, magnetosphere; Aurorae; Ultraviolet observations

Corresponding Author: Dr. Aikaterini Radioti,

Corresponding Author's Institution: Laboratoire de Physique Atmosphérique et Planétaire (LPAP),
Université de Liège, Belgium

First Author: Aikaterini Radioti

Order of Authors: Aikaterini Radioti; Denis Grodent; Xianzhe Jia; Jean-Claude Gérard; Bertrand Bonfond; Wayne Pryor; Jacques Gustin; Donald Mitchell; Caitriona Jackman

Manuscript Region of Origin: BELGIUM

Abstract: We present high-resolution Cassini/UVIS (Ultraviolet Imaging Spectrograph) observations of Saturn's aurora during May 2013 (DOY 140-141). The observations reveal an enhanced auroral activity in the midnight-dawn quadrant in an extended local time sector (~ 02 to 05 LT), which rotates with an average velocity of ~ 45 of rigid corotation. The auroral dawn enhancement reported here, given its observed location and brightness, is most probably due to hot tenuous plasma carried inward in fast moving flux tubes returning from tail reconnection site to the dayside. These flux tubes could generate intense field-aligned currents that would cause aurora to brighten. However, the origin of tail reconnection (solar wind or internally driven) is uncertain. Based on the flux variations, which do not demonstrate flux closure, we suggest that the most plausible scenario is that of internally driven tail reconnection which operates on closed field lines. The observations also reveal multiple intensifications within the enhanced region suggesting an x-line in the tail, which extends from 02 to 05 LT. The localised enhancements evolve in arc and spot-like small scale features, which resemble vortices mainly in the beginning of the sequence. These auroral features could be related to plasma flows enhanced from reconnection which diverge into multiple narrow channels then spread azimuthally and radially. We suggest that the evolution of tail reconnection at Saturn may be pictured by an ensemble of numerous narrow current wedges or that inward transport initiated in the reconnection region could be explained by multiple localised flow burst events. The formation of vortical-like structures could then be related to field-aligned currents, building up in vortical flows in the tail. An alternative, but less plausible, scenario could be that the small scale auroral structures are related to viscous interactions involving small-scale reconnection.

Highlights

- UVIS/Cassini reveals enhanced dawn auroral activity at Saturn
- The auroral dawn enhancement is suggested to be related to magnetotail reconnection
- The observations suggest an x-line which extends from 02 to 05 LT
- Arc and spot-like small scale features are possibly related to plasma flows

High Resolution Copy of Figure 1

[Click here to download High Resolution Copy of Figure: projections_2013_140_without_zoom.eps](#)

High Resolution Copy of Figure 2

[Click here to download High Resolution Copy of Figure: flux_new.eps](#)

High Resolution Copy of Figure 3

[Click here to download High Resolution Copy of Figure: zoom_colortable.eps](#)

We thank the reviewer for the suggestions which we implemented in our manuscript. Please find below the answers to the comments. Changes in the text are highlighted in bold.

Reviewer #1: This is a second revision. The paper is much improved, and I can recommend publication after consideration of the minor comments below:

Line 147: I think that the sub-Mimas longitude needs explicitly indicating since it is nowhere described in the paper.

We added in the text the local time location of the Saturn's moon Mimas to range between 3 and 9 local time (lines 144-149).

Line 151, 153, 169, 267... still many examples of superscript "o" instead of a degree symbol. Also, on line 426, there is a "deg".

Done.

Line 268-271. Whilst I agree that the observations of quasi-constant open flux provide no evidence for flux closure, they do not in themselves provide evidence for an absence of flux closure either. If flux was being opened at the dayside at the same rate that it was being closed in the tail, then one would expect to see no change in open flux content. One might expect to see localised variations in boundary position, and indeed this is seen as explained in lines 252-254. This possibility should be noted.

We agree that the observations of quasi-constant open flux do not provide themselves evidence for an absence of flux closure. We added the following in the text in order to make this point: 'It should be noted that opening of flux at the same rate as it closes would also result in the observed quasi-constant open flux. However, this possibility is less probable because, as mentioned before, this interval does not show any known auroral evidence of low-latitude reconnection which could justify opening of flux.' (lines 264-269)

Also the localized variations in the boundary, which the reviewer mentions, could be possibly attributed to the 1-2 deg dawn-dusk oscillations and should not be confused with flux changes as mentioned in lines 257-261.

Line 319: Should "tight" be "tied" (i.e. related) or do you mean tight as in "very close to"? Either way, it isn't clear.

We changed to 'related'.

Line 348: "auroral" should be "aurora".

Done.

Lines 392 and 428: "planetoward" should be "planetward"

Done.

Line 497: Where you say that the open flux variations "do not demonstrate flux closure", again, they do not explicitly demonstrate an absence if it either. However, if you make this point earlier, as suggested, I think it is fine to leave this statement as it stands in the summary.

We made this point earlier in the text (see answer above) and we left this sentence as it is in the text.

1 A multi-scale magnetotail reconnection event at Saturn
2 and associated flows: Cassini/UVIS observations

3 A. Radioti^a, D. Grodent^a, X. Jia^b, J.-C. Gérard^a, B. Bonfond^a, W. Pryor^c,
4 J. Gustin^a, D. Mitchell^d, C.M. Jackman^e

5 ^a*Laboratoire de Physique Atmosphérique et Planétaire (LPAP), Université de Liège,*
6 *Liège, Belgium.*

7 ^b*Department of Atmospheric, Oceanic, and Space Sciences, University of Michigan, USA*

8 ^c*Science Department, Central Arizona College, Coolidge, Arizona, USA*

9 ^d*Applied Physics Laboratory, Johns Hopkins University, Laurel, Maryland, USA*

10 ^e*School of Physics and Astronomy, University of Southampton, Southampton, England*

11 **Abstract**

12 We present high-resolution Cassini/UVIS (Ultraviolet Imaging Spectro-
13 graph) observations of Saturn's aurora during May 2013 (DOY 140-141). The
14 observations reveal an enhanced auroral activity in the midnight-dawn quad-
15 rant in an extended local time sector (~ 02 to 05 LT), which rotates with an
16 average velocity of $\sim 45\%$ of rigid corotation. The auroral dawn enhancement
17 reported here, given its observed location and brightness, is most probably
18 due to hot tenuous plasma carried inward in fast moving flux tubes returning
19 from a tail reconnection site to the dayside. These flux tubes could generate
20 intense field-aligned currents that would cause aurora to brighten. However,
21 the origin of tail reconnection (solar wind or internally driven) is uncertain.
22 Based mainly on the flux variations, which do not demonstrate flux closure,
23 we suggest that the most plausible scenario is that of internally driven tail re-
24 connection which operates on closed field lines. The observations also reveal
25 multiple intensifications within the enhanced region suggesting an x-line in
26 the tail, which extends from 02 to 05 LT. The localised enhancements evolve
27 in arc and spot-like small scale features, which resemble vortices mainly in
28 the beginning of the sequence. These auroral features could be related to
29 plasma flows enhanced from reconnection which diverge into multiple nar-
30 row channels then spread azimuthally and radially. We suggest that the
31 evolution of tail reconnection at Saturn may be pictured by an ensemble of
32 numerous narrow current wedges or that inward transport initiated in the re-
33 connection region could be explained by multiple localised flow burst events.

34 The formation of vortical-like structures could then be related to field-aligned
35 currents, building up in vortical flows in the tail. An alternative, but less
36 plausible, scenario could be that the small scale auroral structures are related
37 to viscous interactions involving small-scale reconnection.

38 *Keywords:*

39 1. Introduction

40 Saturn's magnetotail is suggested (i.e. Cowley et al. (2005); Jackman
41 et al. (2011)) to be influenced by a combination of solar wind (Dungey,
42 1961) and internally driven (Vasyliūnas, 1983) magnetic reconnection. In the
43 Dungey cycle, reconnected open flux tubes are transported over the poles by
44 the solar wind, before reconnecting in the tail. The newly closed field lines in
45 the tail are then expected to convect around the flanks back to the dayside.
46 The Vasyliūnas cycle is an internally driven process, in which the planet's
47 rapid rotation combined with the mass-loading of flux tubes fed by internal
48 plasma sources (Enceladus and its neutral cloud) lead to reconnection on
49 closed field lines. The closed field lines are then accelerated back to the day-
50 side via the dawn flank. Theoretical studies (Cowley et al., 2005; Badman and
51 Cowley, 2007) and recent global MHD simulations of Saturn's magnetosphere
52 (Jia et al., 2012) suggest that Dungey-type reconnection typically results in
53 hotter and more depleted flux tubes with faster bulk flows from the recon-
54 nection site compared to those produced directly by the Vasyliūnas-cycle recon-
55 nection, mainly due to the different plasma and field conditions of the inflow
56 region surrounding the reconnection site. When only the Vasyliūnas-cycle is
57 operating, such as during intervals of southward IMF, the associated X-line
58 is suggested to form primarily in the midnight to dawn sector. When both
59 processes are at work, the pure Vasyliūnas-cycle X-line is confined to a lim-
60 ited region in the pre-midnight sector while the Dungey-cycle X-line, albeit
61 variable both in space and time, is suggested primarily in the midnight-to-
62 dawn sector, adjacent to the Vasyliūnas-cycle X-line. Additionally, another
63 process which is suggested to influence Saturn's magnetotail is the viscous in-
64 teraction of the solar wind with the planetary magnetosphere, which involves
65 magnetic reconnection on a small scale (Delamere and Bagenal, 2013). The
66 authors propose that mass loading and related viscous boundary processes
67 contribute to the magnetotail structure.

68 The quasi-continuous main auroral emission at Saturn is suggested to

69 be produced by magnetosphere-solar wind interaction, through the shear in
70 rotational flow across the open closed field line boundary (OCFLB) (e.g.
71 Bunce et al. (2008)). Expansion or contraction of the polar cap size, in
72 response to magnetic reconnection, gives evidence on the mechanisms which
73 couple solar wind mass, energy and momentum into the magnetosphere of
74 Saturn (Badman et al., 2005; Radioti et al., 2011; Badman et al., 2014).
75 Low-latitude magnetopause reconnection, which occurs for northward IMF
76 at Saturn, creates new open flux and increases the polar cap size (Cowley
77 et al., 2005; Badman et al., 2005; Jackman and Cowley, 2006; Radioti et al.,
78 2011). Tail reconnection in the Dungey-cycle manner is expected to result in
79 bright and fast rotating aurorae, which expand poleward in the dawn sector,
80 reducing significantly the size of the polar cap and thus resulting in closure
81 of flux (Cowley et al., 2005; Badman et al., 2005; Jia et al., 2012). Finally,
82 tail reconnection on closed field lines (Vasyliūnas-type) is not expected to
83 modify the polar cap size as it does not change the total amount of flux.

84 UV intensification of Saturn’s dawn auroras, together with simultane-
85 ous enhancement of ENA emission and Saturn kilometric radiation (SKR)
86 demonstrated the initiation of several recurrent acceleration events in the
87 midnight to dawn quadrant at radial distances of 15-20 R_S (Mitchell et al.,
88 2009). The authors associated these injection events with reconnection in
89 the tail. Approximately 45 min earlier, localised small scale intensifications,
90 located poleward of the main nightside auroral emission, are suggested to
91 be signatures of dipolarizations in the tail (Jackman et al., 2013). The au-
92 thors suggested that diversion of cross-tail current leads to discrete auroral
93 spots, similar to the terrestrial ‘substorm current wedge’ paradigm (McPher-
94 ron et al., 1973). The small scale intensifications are believed to be precursors
95 to a more intense activity following tail reconnection (Mitchell et al., 2009).
96 A similar event of intense auroral activity in the dawn auroral sector was re-
97 cently observed by the Ultraviolet Imaging Spectrograph (UVIS) instrument
98 on board Cassini. It was characterised by significant flux closure with a rate
99 ranging from 200 to 1000 kV (Radioti et al., 2014). Additionally, Nichols
100 et al. (2014) presented Hubble Space Telescope observations taken in April
101 2013 (DOY 95: 1740 to 1818 UT), which revealed auroral intensifications in
102 the dawn auroral sector, propagating at $\sim 330\%$ rigid corotation from near
103 ~ 01 h LT toward 08 h LT. The authors suggested that these emissions are
104 indicative of ongoing, bursty reconnection of lobe flux in the magnetotail,
105 with flux closure rates of 280 kV. In the same study the authors reported
106 on another similar although less pronounced event which operated between

107 1727 and 1910 UT and on the beginning of a third one between 2053 to 2121
108 UT. Here we present an auroral intensification at Saturn's dawn sector cap-
109 tured by Cassini/UVIS in May 2013 (DOY 140 1942 UT to DOY 141 0100
110 UT), the very beginning of which has also been observed by Hubble Space
111 Telescope (HST) in the aforementioned study.

112 2. Auroral dawn enhancement

113 2.1. UVIS observations on DOY 140-141, 2013

114 Figure 1 shows a sequence of polar projections of Saturn's northern au-
115 rora obtained with the FUV channel (111-191 nm) of the UVIS instrument
116 (Esposito et al., 2004) onboard Cassini on DOY 140-141, 2013. The projec-
117 tions are constructed by combining slit scans, which provide 64 spatial pixels
118 of 1 mrad (along the slit) by 1.5 mrad (across the slit), using the method
119 described by Grodent et al. (2011). Each auroral image, except for the third
120 one (2149 UT - single image), is constructed by adding two subimages show-
121 ing complementary portions of the auroral region taken ~ 30 min apart. The
122 displayed time corresponds to the starting time of the first subimage. During
123 the start of the 1st image and the end of the last image the sub-spacecraft
124 planetocentric latitude increased from 23 to 48 degrees and the spacecraft
125 altitude changed from 5.2 to 5.9 R_S . Because of the relatively high sub-
126 spacecraft latitude, the limb brightening effect is limited and therefore no
127 correction was applied.

128 The auroral emissions reveal an intensification on the main emission (in-
129 cluded in the red rectangle) which starts in the midnight-dawn quadrant. In
130 the first images, it extends from ~ 02 to 05 LT and propagates with time
131 around to 10 LT. This auroral region displays features with a large range of
132 brightness. Localised peaks could be as bright as 30 kR and others could
133 reach values in excess of 300 kR. We determine the velocity of the enhanced
134 auroral feature by tracking the motion of its barycenter. We observe it to
135 rotate with the planet at 56% of rigid corotation at the beginning of the
136 sequence, while its velocity drops to $\sim 27\%$ of rigid corotation at the end.
137 We consider an error bar of $\pm 5\%$ of rigid corotation which corresponds to an
138 uncertainty of 2° (1 pixel) in selecting the border of the enhancement. The
139 mean value of the velocity along the sequence is $\sim 45\%$ of rigid corotation.
140 The morphology of the feature is consistent with the auroral signatures of
141 bursts of tail reconnection discussed in earlier theoretical and observational
142 studies (Cowley et al., 2005; Mitchell et al., 2009; Clarke et al., 2009; Jia

143 et al., 2012; Nichols et al., 2014; Radioti et al., 2014). The major auroral
144 dawn enhancement discussed here is quite bright in several images at **the**
145 **local time location of Mimas, which changes from 3 to 9 local time**
146 **during this interval**. Saturn’s auroral enhancements on the main auro-
147 ral emission are observed to be associated with **the local time location**
148 **of Mimas (and sometimes of Enceladus)** (Pryor (2012); Mitchell et al.
149 (2014b)).

150 In the same sequence, a high latitude ($\sim 80^\circ$) feature is observed between
151 06 and 10 LT, located poleward of the main emission and it is indicated by
152 the yellow arrow. It gradually moves to lower latitudes ($\sim 78^\circ$) and tends
153 to vanish with time. It subcorotates at $\sim 30\%$ of rigid corotation at the be-
154 ginning of the sequence, then its velocity gradually reduces and the feature
155 remains stagnant towards the end of the sequence. This feature could be pos-
156 sibly related to high-latitude reconnection under southward IMF conditions
157 (Gérard et al., 2005; Bunce et al., 2004) and thus it would be on open field
158 lines. Another possibility is that this feature is related to the excess flux of
159 the bursty reconnection of lobe flux in the magnetotail, whose auroral signa-
160 ture is observed by HST between 1727 and 1910 UT (Nichols et al., 2014).
161 This high-latitude feature is observed until the end of the HST sequence at
162 2121 UT.

163 The main emission oval is slightly shifted a couple of degrees during the
164 whole interval namely the afternoon sector shifts to lower latitudes while
165 the pre-dawn region shifts poleward. Previous studies (Nichols et al., 2010)
166 showed that the centers of the auroral ovals at Saturn have been observed
167 to oscillate along an ellipse with a latitudinal amplitude **of 1-2°** due to
168 an external magnetospheric current system. We estimated the direction of
169 the maximum equatorward displacement of the northern hemisphere for our
170 observed interval, based on the azimuthal direction of the effective dipole and
171 according to the method described in Badman et al. (2012). The azimuthal
172 directions of the effective dipoles are taken from the empirical model by
173 Provan et al. (2013). We find that the maximum equatorward displacement
174 of the main emission is directed towards ~ 0.6 LT during the time the second
175 image was taken (start time 2046 UT) while it is directed towards ~ 11 LT
176 when the last image was taken (start time 0100 UT). The direction of the
177 displacement is consistent with our observations.

178 We estimate the flux variations during the observed auroral sequence.
179 For the estimation of the amount of open flux contained within the polar
180 cap region we use a flux function, described in detail in Radioti et al. (2011).

181 The polar cap boundaries are estimated automatically based on the cut-off
182 intensity (4 kR), which corresponds to an average value of the day and night
183 glow emission of this dataset. In our flux estimation we do not include the
184 first image as the UVIS observational geometry provided an incomplete view
185 of the auroral region. For the same reason the local time section between
186 21 and 02 LT in the auroral image taken at 2149 UT is not covered. For
187 this image the calculation of the polar cap boundary at this local time sector
188 is based on the average boundaries from the previous (2046 UT) and next
189 (2253 UT) observations.

190 An example of the selected regions, used to calculate the flux is shown in
191 panel b of Figure 2. The boundaries of all regions of interest are indicated by
192 different symbols. The flux variation of the high latitude emission pointed
193 out by the yellow arrow in Figure 1, whose origin is uncertain (open flux due
194 to high latitude reconnection (Gérard et al., 2005) or excess of closed flux
195 of the bursty reconnection of lobe flux Nichols et al. (2014)) is shown with
196 the orange asterisks in panel a of Figure 2. This flux is observed to decrease
197 with time. We also calculate the total open flux at a given time using two
198 methods. In the first, we calculate the total open flux assuming that the
199 high latitude feature is related to closed flux (excess of closed flux due to tail
200 reconnection) and denote this quantity as 'flux 1'. The 'flux 1' variations as
201 a function of time as well as the boundaries of this region are shown with the
202 blue diamonds in Figure 2 panel a and b, respectively. The open flux 1 values
203 are varying between 20 and 25.5 GWb, which is consistent with the average
204 open flux range (10-50 GWb) estimated based on a large set of HST images
205 (Badman et al., 2014). 'Flux 1' is shown to increase with time from ~ 20 to
206 25.5 GWb within ~ 4 hours, indicative of opening of flux with a reconnection
207 rate of ~ 360 kV ($1 \text{ kV} = 10^{-6} \text{ GWb s}^{-1}$). This rate lies in the extreme upper
208 average reconnection rate range estimated by Badman et al. (2014) and is
209 suggestive of a large dayside reconnection event. Also according to Jackman
210 et al. (2004), which derived dayside reconnection rates from an empirical
211 formula adapted from Earth, 360 kV would correspond to a strong solar wind
212 compression. It should be noted that there is no clear auroral evidence of
213 low latitude dayside reconnection during this observed interval, which could
214 have justified opening of flux. Auroral signatures of dayside reconnection
215 are described as bifurcations of the main emission, namely auroral arcs with
216 one arc attached to the main emission and the other one bending into the
217 polar cap, which are observed in the post-noon local time sector (i.e. as
218 described in Radioti et al. (2011)). These auroral reconnection signatures

219 are accompanied by reconnection voltages of 280 kV. The absence of such
220 features makes the scenario of the total flux to be described by the quantity
221 'flux 1' less valid. In the second method, we calculate the total open flux
222 assuming that the high latitude feature is on open field lines (high latitude
223 reconnection), and denote this quantity as 'flux 2'. In that case the boundary
224 used to estimate the open 'flux 2' is drawn on the auroral emission in panel b
225 by the red line. 'Flux 2' remains almost constant with time (red line Figure
226 2 panel a), while in the second part of the sequence it slightly increases (6%).
227 The open flux 2 values are varying between 26 and 28 GWb, which is within
228 the average open flux range (Badman et al., 2014).

229 The polar cap boundaries are estimated based on 4 kR cut-off intensity,
230 which corresponds to the average value of the day and night glow emission
231 of this dataset, as explained above. In order to test the significance of this
232 threshold on the flux variations, we also estimate the flux for different thresh-
233 olds: 3 and 5 kR (red dashed lines for 'flux 2'). It is demonstrated that while
234 the net amount of open 'flux 2' changes depending on the chosen threshold,
235 the open flux variation as a function of time has a similar trend whatever the
236 initial threshold. We also drew error bars on the 'flux 2', which are estimated
237 by randomly varying the auroral detection threshold from 3 to 5 kR for each
238 local time. This variation range corresponds to Poisson error related to the
239 number of counts included in our initial chosen threshold of 4 kR. The small
240 variations of the 'flux 2' as a function of time are within the error bar.

241 *2.2. On the origin of the auroral enhancement*

242 The auroral brightening in the dawn region can be due to hot tenuous
243 plasma carried inward in fast moving flux tubes returning from tail recon-
244 nection site to the dayside. Such flux tubes may generate intense field-aligned
245 currents that would cause aurora to brighten. Judging only from the ex-
246 pansion of the dawn auroral emission poleward, during the first hour of the
247 sequence, one could argue that the auroral enhancement is evidence of flux
248 closure and thus it is possibly related to tail reconnection which closes flux
249 (Dungey-type). As the UVIS auroral observations do not allow us to esti-
250 mate the open flux at the beginning of the sequence, we can not be certain
251 on the origin of the event. However, from 2046 to 2253 UT and while the
252 auroral dawn emission intensifies and grows spatially with time, one would
253 expect ongoing closure of open flux for a Dungey-type reconnection driven
254 event. Instead the open flux estimations (blue diamonds and red line on Fig-
255 ure 2) demonstrate that the amount of open flux remains almost constant

256 (flux 2) or increases (flux 1) with time, depending on how one interprets the
257 high-latitude feature. The shift of the main emission oval as described above
258 (the afternoon sector shifts to lower latitudes while the pre-dawn region shifts
259 poleward) which could be possibly attributed to the $1\text{-}2^\circ$ dawn-dusk oscillations
260 (Nichols et al., 2010) should not be confused with flux changes (closure
261 or opening of flux). Given the estimated flux variations we suggest that
262 the auroral dawn enhancement under study could be caused by internally
263 driven reconnection, as the Dungey-type (solar wind driven) reconnection
264 process would result in flux closure. **It should be noted that opening of
265 flux at the same rate as it closes would also result in the observed
266 quasi-constant open flux. However, this possibility is less proba-
267 ble because, as mentioned before, this interval does not show any
268 known auroral evidence of low-latitude reconnection which could
269 justify opening of flux.**

270 This event differs from a number of earlier studies in which auroral dawn
271 enhancements are associated with tail reconnection, which closes open flux
272 (Dungey-type tail reconnection) with rates between 200 kV and 1000 kV.
273 Radioti et al. (2014) using the same method presented here, showed that
274 intensifications in the dawn sector in a UVIS sequence are indicative of a
275 flux closure rate which increases from 200 kV to 1000 kV within a couple
276 of hours. During the last interval the open magnetic flux decreased from
277 34.5 to 31 GWb within ~ 1 hour, corresponding to a reconnection rate of
278 ~ 1000 kV. Nichols et al. (2014) estimated a reconnection voltage of ~ 280
279 kV corresponding to dawn enhancements during an HST sequence, based on
280 the poleward propagation of the emission. Statistical analysis of HST auroral
281 emissions were suggestive of tail reconnection flux closure rates ranging from
282 a few tens of kV to 275 kV (Badman et al., 2014). The auroral enhancements
283 in the dawn sector presented by Mitchell et al. (2009) did not include flux
284 estimations and thus it was uncertain whether they were triggered by Dungey
285 or Vasyliūnas type tail reconnection. Tail reconnection flux closure rates
286 estimated based on magnetic field observations at Saturn range from 50 kV to
287 450 kV in strong solar wind compressions, while during short and active solar
288 wind intervals this rate might be significantly higher (Jackman et al., 2004).
289 Finally, based on observations of a post-plasmoid plasma sheet (Richardson
290 et al., 1987) magnetic signature following plasmoid release at Saturn, it is
291 estimated that 0.26-2.2 GWb of flux may be closed via tail reconnection over
292 27 minutes (Jackman et al., 2014).

293 Vasyliūnas type reconnection on closed field lines does not change the

294 amount of open flux and the size of the polar cap. In the absence of Dungey
295 type nightside reconnection, the Vasyliūnas reconnection x-line is expected
296 to form primarily in the midnight to dawn sector (Jia et al., 2012; Cowley
297 et al., 2005), consistent with present observations. However, the location of
298 the auroral enhancement cannot be used as a determining criterion regarding
299 the origin of the event but rather as supporting evidence, since the auroral
300 signature of Dungey-type tail reconnection is also expected to be located in
301 the same region (Cowley et al., 2005; Nichols et al., 2014; Radioti et al.,
302 2014).

303 The rotation velocity of the enhanced region is observed to be 56% of rigid
304 corotation in the beginning of the sequence and is observed to decrease with
305 time up to 27% towards the end. The mean velocity is $\sim 45\%$ of rigid corota-
306 tion, which is consistent with the predictions of MHD simulations (Jia et al.,
307 2012) for auroral signatures of Vasyliūnas-type reconnection. The simulations
308 suggest that, even though the details may vary from case to case depending
309 on the state of the magnetosphere, the intensification of field-aligned currents
310 in the ionosphere associated with Dungey reconnection rotates at an aver-
311 age rate close to or even above rigid corotation between post-midnight and
312 noon sector, while for Vasyliūnas-type, the auroral feature typically rotates
313 at $\sim 50\%$ rigid corotation on average, which is within the range of rotation
314 rate in our observations. The difference in the outflow velocities between Va-
315 syliūnas-type and Dungey-type reconnection is **related** to the Alfvén speed
316 in the inflow region at the reconnection site. For Vasyliūnas-type reconec-
317 tion, which involves mostly reconnection on closed plasma sheet field lines,
318 the inflow Alfvén speed is generally smaller (of the order of 100 km/s). For
319 Dungey-type (or solar wind driven) reconnection, field lines in the tail lobes
320 also participate in the reconnection and thus Alfvén speed on those field lines
321 is generally very high (of the order of 1000 km/s) because of the low densi-
322 ties in the lobes. Indeed, auroral enhancements related to Dungey-type tail
323 reconnection are observed to rotate with higher velocities of $\sim 70\%$ (Radioti
324 et al., 2014) and in some cases Dungey-type auroral bursts (open-flux clo-
325 sure events) may reach extremely high velocities ($\sim 330\%$ rigid corotation)
326 (Nichols et al., 2014).

327 Finally, the brightness of the dawn enhancement as mentioned above, dis-
328 plays features with a large range of brightness. Localised peaks could be as
329 bright as 30 kR and others could reach values in excess of 300 kR. MHD sim-
330 ulations (Jia et al., 2012), suggest that Dungey-type reconnection typically
331 results in hotter and more depleted flux tubes compared to those produced

332 directly by the Vasyliūnas-type reconnection. The brightness values observed
 333 within this enhancement are inconclusive regarding the origin of the event.
 334 The upper range of localised peaks observed here (> 100 kR) is of the same
 335 order of magnitude with events attributed to solar-wind driven tail recon-
 336 nection (Nichols et al., 2014; Radioti et al., 2014), while the localised less
 337 bright features (< 100 kR) are consistent with internally driven reconnection
 338 events.

339 The auroral dawn enhancement reported here, given its observed loca-
 340 tion and brightness, is most probably due to hot tenuous plasma carried
 341 inward in fast moving flux tubes returning from a tail reconnection site to
 342 the dayside. These flux tubes could generate intense field-aligned currents
 343 that would cause aurora to brighten. However, whether this event is solar
 344 wind or internally driven is uncertain. Based on the flux variations, which do
 345 not demonstrate flux closure, we propose that the dawn enhancement is re-
 346 lated to internally driven tail reconnection (Vasyliūnas-type) which operates
 347 on closed field lines. This is also supported by the location of the enhance-
 348 ment in the midnight-dawn quadrant (even though this alone can not prove
 349 the origin of the event as explained above) and the relative low rotational ve-
 350 locity of the event, which are both in accordance with the expectations of the
 351 auroral counterpart of Vasyliūnas-type tail reconnection events, according to
 352 MHD simulations (Jia et al., 2012).

353 **3. Small scale structures within the large auroral enhancement**

354 *3.1. Dipolarization signatures, auroral vortices and streamers*

355 During reconnection and associated dipolarization of the field, the inner
 356 edge of this tail current can be diverted through the ionosphere, in a situa-
 357 tion analogous to the 'substorm current wedge' picture at Earth (McPherron
 358 et al., 1973). Close ups of the dawn enhancements shown in Figure 3, ob-
 359 tained from UVIS high-resolution images (panel a) indicate repetitive mul-
 360 tiple intensifications on the main emission (image taken at 1942 UT) with
 361 spatial dimensions of $\sim 1.5^\circ$ latitude $\times 5^\circ$ longitude and brightness ranging
 362 from 20 to 40 kR. We magnetically map the auroral features on the equatorial
 363 plane using a current sheet model, considering a current sheet half thickness
 364 of $2.5 R_S$, a magnetopause standoff distance of 22 and $27 R_S$, consistent with
 365 Achilleos et al. (2008) inner and outer magnetopause boundary position, and
 366 the current sheet scaling laws from Bunce et al. (2007). Their location in
 367 the equatorial plane lies between 16 and $19 R_S$ and between 19 and $23 R_S$

368 for magnetopause boundary position 22 and 27 R_S , respectively. For the
 369 mapping we consider the latitudinal shift due to the aforementioned oscil-
 370 lations of the center of the main emission oval. These intensifications could
 371 be signatures of dipolarization and thus the onset of reconnection. This is
 372 consistent with previous studies (Jackman et al., 2013) which interpreted
 373 a similar spot-like intensification ($\sim 3^\circ$ latitude $\times 9^\circ$ longitude, maximum
 374 brightness of 16 - 35 kR, equatorial mapped location between ~ 10 and 13
 375 R_S) in the nightside sector as signature of dipolarization in the tail and the
 376 precursor to a more intense activity following tail reconnection. The recon-
 377 nection x-line has been estimated to lie, on average, in the region of ~ 20
 378 to 30 R_S (Mitchell et al., 2005) based on Energetic Neutral Atom (ENA)
 379 emissions linked to reconnection events, which is somewhat further than our
 380 auroral intensifications. Also modelling work has suggested the position of
 381 the x-line to be highly sensitive to solar wind conditions and to vary from
 382 25 to 40 R_S (Jia et al., 2012). In addition, a recent study (Jackman et al.,
 383 2014) suggested that the position of the x-line might be highly mobile, as
 384 there is no clear demarcation between the **planetward** and tailward events.
 385 Our observations are also indicative of multiple reconnection onsets along an
 386 extended x-line from ~ 02 to 05 LT. We propose that tail reconnection at
 387 Saturn may take the form of multiple x-lines in the tail, by analogy with
 388 the Earth (Imber et al., 2011), even though in the terrestrial case it was
 389 suggested that the x-line is also extended in radial distance.

390 The observations reveal that soon after onset (images taken from 2046
 391 UT to the end), the intensifications evolve with time into a series of spot-
 392 and arc-like structures. The arc-like structures observed at Saturn could be
 393 related to flows released from reconnection similar to the auroral streamers
 394 at Earth (i.e. Angelopoulos et al. (1996); Sergeev et al. (2004)). Auroral
 395 streamers have been related to enhanced earthward flows within the plasma
 396 sheet and to magnetic field dipolarizations, which connect to the ionosphere
 397 via field-aligned currents following the concept of a narrow current wedge
 398 (Birn et al., 2004). Similar auroral features have been related to inward
 399 moving flows released after tail reconnection at Jupiter (Radioti et al., 2010).
 400 If this is also the case at Saturn, then these observations would be suggestive
 401 of multiple narrow channels spread azimuthally and radially.

402 The small scale features occasionally resemble vortices, a picture that is
 403 especially evident in the image taken at 2149 UT in Figure 3. The forma-
 404 tion of flow vorticity and associated FAC generation at Earth is predicted
 405 by several alternative scenarios related to substorms, such as plasma flow

406 breaking (e.g., Shiokawa et al. (1997)) cross-field current instability (e.g.,
407 Lui et al. (1991)) and ballooning instabilities (e.g., Voronkov et al. (1997)).
408 Auroral vortices surrounded by streamers have also been reported after sub-
409 storm reconnection onset at Earth (Lyons et al., 2013), very similar to the
410 observations shown here. Keiling et al. (2009), based on multi-spacecraft
411 observations, suggested that space vortices generated the field-aligned cur-
412 rent of the current wedge at the beginning of the substorm expansion phase
413 and coupled to the ionosphere causing ionospheric vortices, according to the
414 concept proposed by Birn et al. (2004).

415 Cassini plasma observations have shown evidence of numerous significant
416 inflow events in the postmidnight sector following tail reconnection at Saturn
417 (Thomsen et al., 2013). The large majority of the plasma flows are found
418 to be within 20° of the corotation direction, though with flow speeds signif-
419 icantly lower than full corotation. Also fast (brief episodes of ~ 10 minutes)
420 **planetward** convective flows have been observed by the energetic particle
421 detector onboard Cassini in the nightside magnetosphere (Mitchell et al.,
422 2014a). They have been identified as transitional events between current
423 sheet collapse and interchange. The brief periods of radial flow could set up
424 vortical flow at their boundaries, assuming they are limited in azimuth. The
425 simulations by Jia et al. (2012) predict fast plasma flows, released from tail
426 reconnection at Saturn, to move towards the planet and create flow shear
427 with the surroundings. Those rapidly moving flux tubes are expected to
428 generate strong disturbances in the ionosphere. We suggest that the concept
429 proposed by Birn et al. (2004) for the Earth might also be applicable to Sat-
430 urn. Figure 3, panel b presents an illustration of the build up of field-aligned
431 currents by vortex flow in the tail which could explain the formation of auro-
432 ral vortices and streamers during dipolarization current wedge (adapted from
433 Birn et al. (2004)). According to this model, planetward moving flow pushes
434 the neighbouring field lines and causes a twist or shear in the magnetic field.

435 Finally, our results indicate that the evolution of tail reconnection at
436 Saturn may not be pictured with a single current wedge. Instead the multiple
437 intensifications and streamers indicate that the evolution of tail reconnection
438 can be explained by an ensemble of many narrow current wedges or that
439 inward transport related to the reconnection region could be explained by
440 multiple localised flow burst events in analogy to the terrestrial case (e.g.
441 Nakamura et al. (1994); Lyons et al. (2013)).

442 *3.2. Auroral signatures of viscous interaction of the solar wind with the mag-*
443 *netosphere*

444 Alternatively to the aforementioned interpretation, one could suggest that
445 the dawn small scale features observed here are auroral signatures of viscous
446 interaction of the solar wind with the magnetosphere. Delamere and Bagenal
447 (2013) proposed that viscous interaction involves magnetic reconnection on a
448 small scale, thus facilitating intermittent reconnection. Cassini observations
449 of a plasma vortex in Saturn’s dayside outer magnetosphere were sugges-
450 tive of the presence of nonlinear Kelvin-Helmholtz instability at Saturn’s
451 morning magnetospheric boundaries (Masters et al., 2010). However, recent
452 global survey based on Cassini data from 2004 to 2009 revealed that most of
453 the potential Kelvin-Helmholtz activity is on the dusk flank (Delamere et al.,
454 2013). Masters et al. (2010) proposed that plasma vortices related to Kelvin-
455 Helmholtz instability could result in the formation of field-aligned current
456 systems which could give rise to vortex footprints in the ionosphere. Small
457 scale structures on the main UV emission located at noon and in dusk sector
458 have been previously reported (Grodent et al., 2011) and are related to pat-
459 terns of upward field-aligned currents resulting from non-uniform plasma flow
460 in the equatorial plane possibly triggered by magnetopause Kelvin-Helmholtz
461 waves. These auroral features had brightness up to 30 kR and were not part
462 of a major auroral enhancement, while the observations here are indicative of
463 much brighter small scale features (up to 300 kR). Additionally, the observed
464 emissions are confined to the dawn sector while most of the potential Kelvin-
465 Helmholtz activity is on the dusk flank according to Delamere et al. (2013).
466 Therefore we suggest that it is less plausible that the present observations
467 bear a signature of viscous interaction involving magnetic reconnection on
468 small scale such as proposed by Delamere and Bagenal (2013).

469 **4. Summary and conclusions**

470 We present high-resolution UVIS observations of Saturn’s aurora during
471 the DOY 140-141, 2013. The observations reveal an enhanced activity in
472 the midnight-dawn quadrant. The region extends from ~ 02 to 05 LT and
473 propagates with time up to 10 LT. It has an average brightness of ~ 150
474 kR, while it rotates with an average velocity of $\sim 45\%$ of rigid corotation.
475 The morphology of the feature is consistent with the auroral signatures of
476 bursts of tail reconnection discussed in earlier theoretical and observational
477 studies (Cowley et al., 2005; Mitchell et al., 2009; Clarke et al., 2009; Jia

478 et al., 2012; Nichols et al., 2014; Radioti et al., 2014). Given its observed
479 location and brightness, it is most probably due to hot tenuous plasma carried
480 inward in fast moving flux tubes returning from tail reconnection site to the
481 dayside. These flux tubes could generate intense field-aligned currents that
482 would cause aurora to brighten. Whether this event is attributed to solar
483 wind (Dungey-type) or internally driven (Vasyliūnas-type) reconnection is
484 uncertain. However, based on the open flux variations during this sequence
485 (red line on Figure 2), which do not demonstrate flux closure, the event is
486 possibly indicative of Vasyliūnas type reconnection on closed field lines which
487 does not modify the amount of open flux. In the absence of Dungey type
488 nightside reconnection, which could be the case for a period of southward
489 IMF, the Vasyliūnas reconnection x-line is expected to form primarily in the
490 midnight to dawn sector (Jia et al., 2012; Cowley et al., 2005) in accordance
491 with our observations. Additionally, the rotation velocity of the enhanced
492 region is observed to be on average $\sim 45\%$ of rigid corotation, which is
493 consistent with the predictions of MHD simulations (Jia et al., 2012) for
494 auroral signatures of Vasyliūnas-type reconnection. The auroral signature
495 associated with Dungey type reconnection rotates at much larger average
496 rates close to or even above rigid corotation. It should be noted, however,
497 that the brightness of the dawn enhancement is inconclusive regarding the
498 origin of the event, since the enhancement region exhibits localised peaks
499 with a large range of brightness, which could be attributed to both types of
500 tail reconnection.

501 Our observations also reveal multiple intensifications indicative of an x-
502 line in the tail which extends from 02 to 05 LT. The localised enhancements
503 evolve in arc and spot-like features, which resemble vortices mainly in the
504 beginning of the sequence. These features could be related to flows released
505 from reconnection that are separated into multiple narrow channels spread
506 azimuthally and radially. We suggest that the evolution of tail reconnection
507 at Saturn may not be pictured by a single current wedge. Instead the multiple
508 intensifications and substructures indicate that the evolution of tail recon-
509 nection can be explained by an ensemble of many narrow current wedges or
510 that inward transport related to the reconnection region could be explained
511 by multiple localised flow bursts events similar to the picture proposed for
512 Earth (Nakamura et al., 1994; Lyons et al., 2013). Although the reason for
513 the formation of vortical-like structures remains unknown, one possibility
514 could be that they are attributed to field-aligned currents, which are build
515 up by vortex flow in the tail (Birn et al., 2004). A less plausible scenario

516 could be that the small scale structures are related to viscous interactions
517 involving small-scale reconnection.

518 **acknowledgments**

519 This work is based on observations with the UVIS instrument onboard
520 the NASA/ESA Cassini spacecraft. The research was supported by (F.R.S. -
521 FNRS) and the PRODEX Program managed by the European Space Agency
522 in collaboration with the Belgian Federal Science Policy Office. B.B. is
523 funded by FNRS. X.J. acknowledges the support by NASA through grant
524 NNX12AK34G and by the Cassini mission under contract JPL 1409449.
525 CMJ's work at Southampton is supported by a Science and Technology
526 Facilities Council Ernest Rutherford Fellowship. A.R. gratefully acknowl-
527 edges Gabrielle Provan for providing the azimuthal directions of the effective
528 dipoles.

529 **References**

- 530 Achilleos, N., Arridge, C.S., Bertucci, C., Jackman, C.M., Dougherty, M.K.,
531 Khurana, K.K., Russell, C.T., 2008. Large-scale dynamics of Saturn's
532 magnetopause: Observations by Cassini. *Journal of Geophysical Research*
533 (Space Physics) 113, 11209.
- 534 Angelopoulos, V., Coroniti, F.V., Kennel, C.F., Kivelson, M.G., Walker,
535 R.J., Russell, C.T., McPherron, R.L., Sanchez, E., Meng, C.I., Baumjo-
536 hann, W., Reeves, G.D., Belian, R.D., Sato, N., Friis-Christensen, E.,
537 Sutcliffe, P.R., et al., 1996. Multipoint analysis of a bursty bulk flow event
538 on April 11, 1985. *Journal of Geophysical Research* 101, 4966–4990.
- 539 Badman, S.V., Andrews, D.J., Cowley, S.W.H., Lamy, L., Provan, G., Tao,
540 C., Kasahara, S., Kimura, T., Fujimoto, M., Melin, H., Stallard, T.,
541 Brown, R.H., Baines, K.H., 2012. Rotational modulation and local time
542 dependence of Saturn's infrared H₃⁺ auroral intensity. *Journal of Geo-*
543 *physical Research (Space Physics)* 117, 9228.
- 544 Badman, S.V., Bunce, E.J., Clarke, J.T., Cowley, S.W.H., GéRard, J.C.,
545 Grodent, D., Milan, S.E., 2005. Open flux estimates in Saturn's magneto-
546 sphere during the January 2004 Cassini-HST campaign, and implications
547 for reconnection rates. *Journal of Geophysical Research (Space Physics)*
548 110, 11216.

- 549 Badman, S.V., Cowley, S.W.H., 2007. Significance of Dungey-cycle flows in
550 Jupiter's and Saturn's magnetospheres, and their identification on closed
551 equatorial field lines. *Annales Geophysicae* 25, 941–951.
- 552 Badman, S.V., Jackman, C.M., Nichols, J.D., Clarke, J.T., Gérard, J.C.,
553 2014. Open flux in Saturn's magnetosphere. *Icarus* 231, 137–145.
- 554 Birn, J., Raeder, J., Wang, Y., Wolf, R., Hesse, M., 2004. On the propagation
555 of bubbles in the geomagnetic tail. *Annales Geophysicae* 22, 1773–1786.
- 556 Bunce, E.J., Arridge, C.S., Clarke, J.T., Coates, A.J., Cowley, S.W.H.,
557 Dougherty, M.K., Gérard, J.C., Grodent, D., Hansen, K.C., Nichols, J.D.,
558 Southwood, D.J., Talboys, D.L., 2008. Origin of Saturn's aurora: Simul-
559 taneous observations by Cassini and the Hubble Space Telescope. *Journal*
560 *of Geophysical Research (Space Physics)* 113, 9209.
- 561 Bunce, E.J., Cowley, S.W.H., Alexeev, I.I., Arridge, C.S., Dougherty, M.K.,
562 Nichols, J.D., Russell, C.T., 2007. Cassini observations of the variation of
563 Saturn's ring current parameters with system size. *Journal of Geophysical*
564 *Research (Space Physics)* 112, 10202.
- 565 Bunce, E.J., Cowley, S.W.H., Yeoman, T.K., 2004. Jovian cusp processes:
566 Implications for the polar aurora. *Journal of Geophysical Research (Space*
567 *Physics)* 109, 9.
- 568 Clarke, J.T., Nichols, J., Gérard, J.C., Grodent, D., Hansen, K.C., Kurth,
569 W., Gladstone, G.R., Duval, J., Wannawichian, S., Bunce, E., Cowley,
570 S.W.H., Crary, F., Dougherty, M., Lamy, L., Mitchell, D., Pryor, W.,
571 Retherford, K., Stallard, T., Zieger, B., Zarka, P., Cecconi, B., 2009. Re-
572 sponse of Jupiter's and Saturn's auroral activity to the solar wind. *Journal*
573 *of Geophysical Research (Space Physics)* 114, 5210.
- 574 Cowley, S.W.H., Badman, S.V., Bunce, E.J., Clarke, J.T., Gérard, J.C.,
575 Grodent, D., Jackman, C.M., Milan, S.E., Yeoman, T.K., 2005. Recon-
576 nection in a rotation-dominated magnetosphere and its relation to Saturn's
577 auroral dynamics. *Journal of Geophysical Research (Space Physics)* 110,
578 2201.
- 579 Delamere, P.A., Bagenal, F., 2013. Magnetotail structure of the giant mag-
580 netospheres: Implications of the viscous interaction with the solar wind.
581 *Journal of Geophysical Research (Space Physics)* 118, 7045–7053.

- 582 Delamere, P.A., Wilson, R.J., Eriksson, S., Bagenal, F., 2013. Magnetic
583 signatures of Kelvin-Helmholtz vortices on Saturn’s magnetopause: Global
584 survey. *Journal of Geophysical Research (Space Physics)* 118, 393–404.
- 585 Dungey, J.W., 1961. Interplanetary magnetic field and the auroral zones.
586 *Physical Review Letters* .
- 587 Esposito, L.W., Barth, C.A., Colwell, J.E., Lawrence, G.M., McClintock,
588 W.E., Stewart, A.I.F., Keller, H.U., Korth, A., Lauche, H., Festou, M.C.,
589 Lane, A.L., Hansen, C.J., Maki, J.N., West, R.A., Jahn, H., Reulke, R.,
590 Warlich, K., Shemansky, D.E., Yung, Y.L., 2004. The Cassini Ultraviolet
591 Imaging Spectrograph Investigation. *Space Science Review* 115, 299–361.
- 592 Gérard, J.C., Bunce, E.J., Grodent, D., Cowley, S.W.H., Clarke, J.T., Bad-
593 man, S.V., 2005. Signature of Saturn’s auroral cusp: Simultaneous Hubble
594 Space Telescope FUV observations and upstream solar wind monitoring.
595 *Journal of Geophysical Research (Space Physics)* 110, 11201.
- 596 Grodent, D., Gustin, J., Gérard, J.C., Radioti, A., Bonfond, B., Pryor, W.R.,
597 2011. Small-scale structures in Saturn’s ultraviolet aurora. *Journal of*
598 *Geophysical Research (Space Physics)* 116, 9225.
- 599 Imber, S.M., Slavin, J.A., Auster, H.U., Angelopoulos, V., 2011. A THEMIS
600 survey of flux ropes and traveling compression regions: Location of the
601 near-Earth reconnection site during solar minimum. *Journal of Geophys-
602 ical Research (Space Physics)* 116, 2201.
- 603 Jackman, C.M., Achilleos, N., Bunce, E.J., Cowley, S.W.H., Dougherty,
604 M.K., Jones, G.H., Milan, S.E., Smith, E.J., 2004. Interplanetary mag-
605 netic field at 9 AU during the declining phase of the solar cycle and its
606 implications for Saturn’s magnetospheric dynamics. *Journal of Geophys-
607 ical Research (Space Physics)* 109, 11203.
- 608 Jackman, C.M., Achilleos, N., Cowley, S.W.H., Bunce, E.J., Radioti, A.,
609 Grodent, D., Badman, S.V., Dougherty, M.K., Pryor, W., 2013. Auroral
610 counterpart of magnetic field dipolarizations in Saturn’s tail. *Planetary
611 and Space Science* 82, 34–42.
- 612 Jackman, C.M., Cowley, S.W.H., 2006. A model of the plasma flow and
613 current in Saturn’s polar ionosphere under conditions of strong Dungey
614 cycle driving. *Annales Geophysicae* 24, 1029–1055.

- 615 Jackman, C.M., Slavin, J.A., Cowley, S.W.H., 2011. Cassini observations
616 of plasmoid structure and dynamics: Implications for the role of magnetic
617 reconnection in magnetospheric circulation at Saturn. *Journal of Geophys-*
618 *ical Research (Space Physics)* 116, 10212.
- 619 Jackman, C.M., Slavin, J.A., Kivelson, M.G., Southwood, D.J., Achilleos,
620 N., Thomsen, M.F., DiBraccio, G.A., Eastwood, J.P., Freeman, M.P.,
621 Dougherty, M.K., Vogt, M.F., 2014. Saturn's dynamic magnetotail: A
622 comprehensive magnetic field and plasma survey of plasmoids and travel-
623 ing compression regions and their role in global magnetospheric dynamics.
624 *Journal of Geophysical Research (Space Physics)* 119, 5465–5494.
- 625 Jia, X., Hansen, K.C., Gombosi, T.I., Kivelson, M.G., Tóth, G., DeZeeuw,
626 D.L., Ridley, A.J., 2012. Magnetospheric configuration and dynamics of
627 Saturn's magnetosphere: A global MHD simulation. *Journal of Geophysic-*
628 *cal Research (Space Physics)* 117, 5225.
- 629 Keiling, A., Angelopoulos, V., Runov, A., Weygand, J., Apatenkov, S.V.,
630 Mende, S., McFadden, J., Larson, D., Amm, O., Glassmeier, K.H., Auster,
631 H.U., 2009. Substorm current wedge driven by plasma flow vortices:
632 THEMIS observations. *Journal of Geophysical Research (Space Physics)*
633 114, 0.
- 634 Lui, A.T.Y., Chang, C.L., Mankofsky, A., Wong, H.K., Winske, D., 1991.
635 A cross-field current instability for substorm expansions. *Journal of Geo-*
636 *physical Research* 96, 11389.
- 637 Lyons, L.R., Nishimura, Y., Donovan, E., Angelopoulos, V., 2013. Dis-
638 tinction between auroral substorm onset and traditional ground magnetic
639 onset signatures. *Journal of Geophysical Research (Space Physics)* 118,
640 4080–4092.
- 641 Masters, A., Achilleos, N., Kivelson, M.G., Sergis, N., Dougherty, M.K.,
642 Thomsen, M.F., Arridge, C.S., Krimigis, S.M., McAndrews, H.J., Kanani,
643 S.J., Krupp, N., Coates, A.J., 2010. Cassini observations of a Kelvin-
644 Helmholtz vortex in Saturn's outer magnetosphere. *Journal of Geophysical*
645 *Research (Space Physics)* 115, 7225.
- 646 McPherron, R.L., Russell, C.T., Aubry, M.P., 1973. Satellite studies of
647 magnetospheric substorms on August 15, 1968: 9. Phenomenological model
648 for substorms. *Journal of Geophysical Research* 78, 3131.

- 649 Mitchell, D.G., Brandt, P.C., Carbary, J.F., Kurth, W.S., Krimigis, S.M.,
650 Paranicas, C., Krupp, N., Hamilton, D.C., Mauk, B.H., Hospodarsky,
651 G.B., Dougherty, M.K., Pryor, W.R., 2014a. Injection, Interchange, and
652 Reconnection: Energetic Particle Observations in Saturn's Magnetosphere.
653 Magnetotail in the Solar System, Geophysical Monograph .
- 654 Mitchell, D.G., Brandt, P.C., Roelof, E.C., Dandouras, J., Krimigis, S.M.,
655 Mauk, B.H., Paranicas, C.P., Krupp, N., Hamilton, D.C., Kurth, W.S.,
656 Zarka, P., Dougherty, M.K., Bunce, E.J., Shemansky, D.E., 2005. En-
657 ergetic ion acceleration in Saturn's magnetotail: Substorms at Saturn?
658 Geophysical Research Letters 32, 20.
- 659 Mitchell, D.G., Carbary, J.F., Bunce, E.J., Radioti, A., Badman, S.V., Pryor,
660 W.R., Hospodarsky, G.B., Kurth, W.S., 2014b. Recurrent Pulsations in
661 Saturn's High Latitude Magnetosphere. *Icarus* .
- 662 Mitchell, D.G., Krimigis, S.M., Paranicas, C., Brandt, P.C., Carbary, J.F.,
663 Roelof, E.C., Kurth, W.S., Gurnett, D.A., Clarke, J.T., Nichols, J.D.,
664 Gérard, J.C., Grodent, D.C., Dougherty, M.K., Pryor, W.R., 2009. Recur-
665 rent energization of plasma in the midnight-to-dawn quadrant of Saturn's
666 magnetosphere, and its relationship to auroral UV and radio emissions.
667 *Planetary and Space Science* 57, 1732–1742.
- 668 Nakamura, R., Baker, D.N., Yamamoto, T., Belian, R.D., Bering, III, E.A.,
669 Benbrook, J.R., Theall, J.R., 1994. Particle and field signatures during
670 pseudobreakup and major expansion onset. *Journal of Geophysical Re-*
671 *search* 99, 207–221.
- 672 Nichols, J.D., Badman, S.V., Baines, K.H., Brown, R.H., Bunce, E.J., Clarke,
673 J.T., Cowley, S.W.H., Crary, F.J., Dougherty, M.K., Gérard, J.C., Gro-
674 cott, A., Grodent, D., Kurth, W.S., Melin, H., Mitchell, D.G., Pryor, W.R.,
675 Stallard, T.S., 2014. Dynamic auroral storms on Saturn as observed by
676 the Hubble Space Telescope. *Geophysical Research Letters* 41, 3323–3330.
- 677 Nichols, J.D., Cowley, S.W.H., Lamy, L., 2010. Dawn-dusk oscillation of
678 Saturn's conjugate auroral ovals. *Geophysical Research Letters* 37, 24102.
- 679 Provan, G., Cowley, S.W.H., Sandhu, J., Andrews, D.J., Dougherty, M.K.,
680 2013. Planetary period magnetic field oscillations in Saturn's magneto-
681 sphere: Postequinox abrupt nonmonotonic transitions to northern system

- 682 dominance. *Journal of Geophysical Research (Space Physics)* 118, 3243–
683 3264.
- 684 Pryor, W. R., e.a., 2012. Ultraviolet auroral pulsations on Saturn from
685 Cassini UVIS, in: DPS 44, Reno, Nevada, Bull. American Astronomical
686 Soc., 44, 5, presentation 413.05.
- 687 Radioti, A., Grodent, D., Gérard, J.C., Bonfond, B., 2010. Auroral signatures
688 of flow bursts released during magnetotail reconnection at Jupiter. *Journal*
689 *of Geophysical Research (Space Physics)* 115, 7214.
- 690 Radioti, A., Grodent, D., Gérard, J.C., Milan, S.E., Bonfond, B., Gustin, J.,
691 Pryor, W., 2011. Bifurcations of the main auroral ring at Saturn: iono-
692 spheric signatures of consecutive reconnection events at the magnetopause.
693 *Journal of Geophysical Research (Space Physics)* 116, 11209.
- 694 Radioti, A., Grodent, D., Gérard, J.C., Milan, S.E., Fear, R.C., Jackman,
695 C.M., Bonfond, B., Pryor, W., 2014. Saturn’s elusive nightside polar arc.
696 *Geophysical Research Letters* .
- 697 Richardson, I.G., Cowley, S.W.H., Hones, Jr., E.W., Bame, S.J., 1987.
698 Plasmoid-associated energetic ion bursts in the deep geomagnetic tail -
699 Properties of plasmoids and the postplasmoid plasma sheet. *Journal of*
700 *Geophysical Research* 92, 9997–10013.
- 701 Sergeev, V., Liou, K., Newell, P., Ohtani, S., Hairston, M., Rich, F., 2004.
702 Auroral streamers: characteristics of associated precipitation, convection
703 and field-aligned currents. *Annales Geophysicae* 22, 537–548.
- 704 Shiokawa, K., Baumjohann, W., Haerendel, G., 1997. Braking of high-speed
705 flows in the near-Earth tail. *Geophysical Research Letters* 24, 1179–1182.
- 706 Thomsen, M.F., Wilson, R.J., Tokar, R.L., Reisenfeld, D.B., Jackman, C.M.,
707 2013. Cassini/CAPS observations of duskside tail dynamics at Saturn.
708 *Journal of Geophysical Research (Space Physics)* 118, 5767–5781.
- 709 Vasyliūnas, V.M., 1983. Plasma distribution and flow. *Physics of the Jovian*
710 *Magnetosphere*, Cambridge Univ. Press.
- 711 Voronkov, I., Rankin, R., Frycz, P., Tikhonchuk, V.T., Samson, J.C., 1997.
712 Coupling of shear flow and pressure gradient instabilities. *Journal of Geo-*
713 *physical Research* 102, 9639–9650.

DOY 2013 140-141

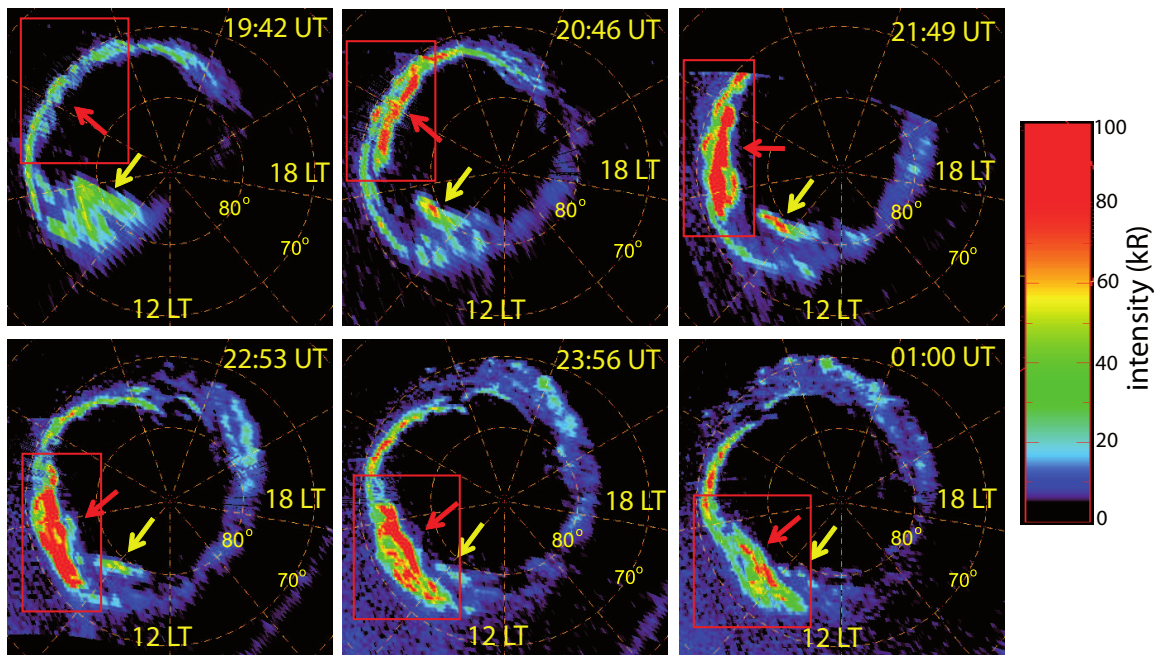


Figure 1: A sequence of polar projections of Saturn's northern aurora obtained with the FUV channel of UVIS onboard Cassini. The first image starts at 1942 UT on DOY 140, 2013 and the last one at 0100 UT on DOY 141, 2013. Noon is to the bottom and dusk to the right. The grid shows latitudes at intervals of 10° and meridians of 40° . The red rectangles include the auroral intensifications in the dawn-midnight quadrant, related to bursts of tail reconnection. Yellow arrows point to an auroral feature that was left over from a previous reconnection event. The color scale is saturated to 100 kR, as shown in the color bar to the right. The polar projection procedure does not preserve photometry; therefore, the colour table may only be used as a proxy for the projected emission brightness.

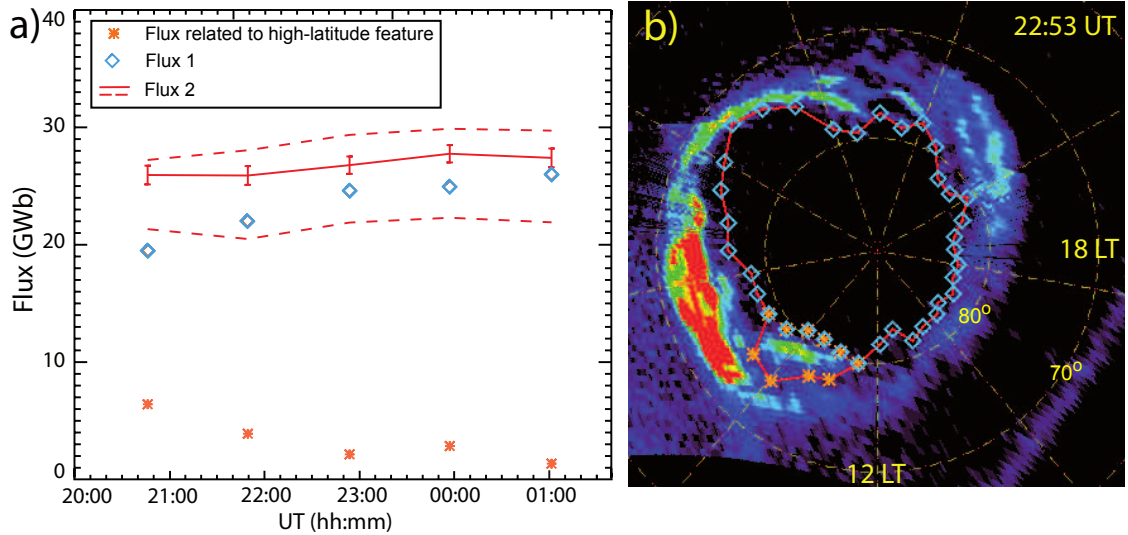


Figure 2: Panel a: Flux variations as a function of time, based on the observed auroral sequence in Figure 1. The polar cap boundaries are estimated automatically based on the cut-off intensity (4 kR), which corresponds to an average value of the day and night glow emission of these observations. The orange asterisks stand for the flux of the high latitude emission pointed out by the yellow arrow in Figure 1, which could be related either to high latitude reconnection (open flux) or excess flux of the bursty reconnection of lobe flux (closed flux). The blue diamonds correspond to 'flux 1', which is the total open flux at a given time assuming that the high latitude feature is related to closed flux. The red line corresponds to 'flux 2', which is the total open flux at a given time considering that the high latitude feature is related to open flux. Red dashed lines correspond to 'flux 2' estimated for the extreme thresholds of 3 kR (bottom line) and 5 kR (top line). The error bars indicate the statistical error related to the number of counts included in our initial chosen threshold of 4 kR. Panel b: A polar projection of Saturn's aurora taken at 2253 UT during the sequence shown in Figure 1. The different symbols draw the boundaries used to derive the different types of flux variations.

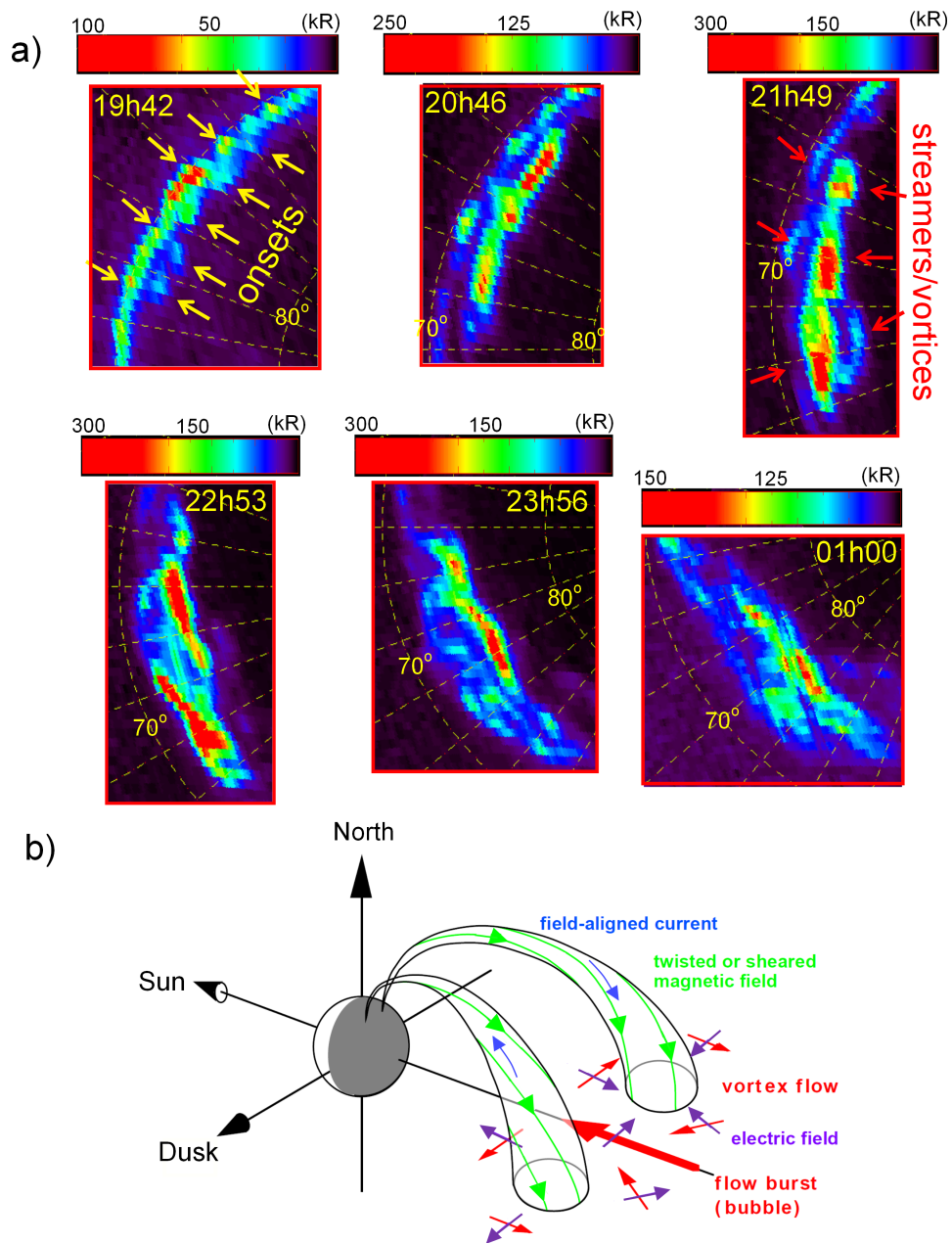


Figure 3: Panel a: Projected close-ups of a selected auroral region, indicated with the red rectangles on the complete projections of Figure 1. A single subimage is used for the close ups. The grid shows meridians of 10° and the latitudes are indicated. Yellow arrows indicate intensifications, which are discussed in the text as reconnection onsets. Red arrows indicate arc- and spot-like structures, which are discussed in the text as streamers and vortices. In order to highlight the details of the auroral structure the colorscale used is different for each panel. The polar projection procedure does not preserve photometry; therefore, the colour table may only be used as a proxy for the projected emission brightness. Panel b: Schematic illustrating the build-up of field-aligned currents by vortex flow in the tail adapted for Saturn from the terrestrial case (Birn et al., 2004).

LaTeX Source Files 1

[Click here to download LaTeX Source Files: multi_scale_reconnection_icarus_revised_2.tex](#)

LaTeX Source Files 2

[Click here to download LaTeX Source Files: my_biblio.bib](#)